Malaysian Journal of Mathematical Sciences 16(3): 517–536 (2022)
https://doi.org/10.47836/mjms.16.3.08

Malaysian Journal of Mathematical Sciences

Journal homepage: https://einspem.upm.edu.my/journal

A Fractional Order SITR Model for Forecasting of Transmission of COVID-19: Sensitivity Statistical Analysis

Al-Zahrani, S. M.[1], Elsmih, F. E. I.[2,3], Al-Zahrani, K. S.[4], and Saber, S. *[2,5]

[1]*Faculty of Arts and Science in Almandaq, Al-Baha University, Saudi Arabia*
[2]*Department of Mathematics, Faculty of Sciences and Arts in Baljurashi, Al-Baha University, Saudi Arabia*
[3]*Department of Mathematics, Faculty of Sciences, Peace University, Sudan*
[4]*Department of Biology, Faculty of Sciences and Arts in Almandaq, Al-Baha University, Saudi Arabia*
[5]*Department of Mathematics and Computer Science, Faculty of Science, Beni-Suef University, Egypt*

E-mail: sayedkay@yahoo.com
**Corresponding author*

Received: 28 January 2022
Accepted: 25 April 2022

Abstract

In this work, we investigate the effects of the contact rate between people on the covid-19 virus transmission through a susceptible-infected-treatment-recovered (SITR) fractional mathematical model. Several strategies are introduced, and the development methodology is constructed up in various cases based on the rate of individual contact, due to confinement and social distancing rules, which can be useful in reducing infection. The existence and uniqueness of the proposed model solution are established, as well as the basic reproduction number. The basic reproduction number has been used to control the dynamics of the fractional SITR model completely, which determines whether or not the infection is extinguished. The global stability of the infection-free balance and endemic equilibrium point of the proposed model has been fully established using the Lyapunov-LaSalle type theorem. Furthermore, a sensitivity analysis is carried out to find out which parameter is the most dominant to affect the disease's endemicity and to see how changes in parameters affect Covid-19's beginning disease transmission. The fractional Adams-Bashforth method is used to compute an iterative solution to the model. Finally, using the model parameter values to explain the importance of the arbitrary fractional-order derivative, the numerical results using MATLAB are presented.

Keywords: COVID-19; mathematical model; endemic-equilibrium; stability analysis.

1 Introduction

Fractional calculus is a widening of the non-integer order of integral and derivative. The first application of fractional calculus was due to Abel in his solution to the Tautocrone problem [1]. As a result, it's used mostly in physics, biology, medicine, viscoelasticity, bioengineering, economics, and control theory [2]-[18]. As compared to the ordinary derivative, which is a local operator, the fractional-order derivative expands the equilibrium field of dynamical systems.

In epidemiology, there has been a lot of work done with fractional-order derivatives. Recent high-profile outbreaks, like those caused by Ebola, Zika, Pandemic influenza, Middle East Respiratory Syndrome (MERS), and COVID-19, have highlighted the global importance of infectious diseases and the need for coordinated efforts to prevent outbreaks. Fractional order models for influenza, dengue fever, malaria, and tuberculosis, for example [19]-[29]. The COVID-19 pandemic has already spread throughout the world and the people are aware of the disease and they are using precautions against the pandemic. But, still, the covid-19 is spreading very quickly. Global efforts begin with a discussion of numerous healthcare solutions to reduce the impact of the current coronavirus on the population (COVID-19). In 2019, a new coronavirus (COVID-19) was found in Wuhan, China. According to WHO, the majority of patients infected with the COVID-19 virus will have a mild to moderate viral infection and will recover without needing any additional treatment. People who are older, as well as those who have underlying health issues like cardiovascular disease, diabetes, chronic respiratory illness, and cancer, are more vulnerable to serious diseases.

It's essential to create a mathematical model to evaluate the coronavirus's transmission dynamics and transmissibility. Many scientists have sought to determine the basic reproduction number $\mathfrak{R}_0$ using ordinary differential equations, or utilizing serial intervals and the intrinsic growth rate [30]-[32]. The number of coronavirus cases in Saudi Arabia was reported to be 547,090 on September 30, 2021, with 536,125 recovered patients and 8,713 deaths. On the other hand, the recovery ratio is greater than the death ratio in terms of numbers. The graphic depicts the number of people who died as a result of COVID-19 in the last 100 days (20 June to 30 September 2021).

To stop the spread of the diseases, a vaccine is needed. But, in absence of the vaccine, people must maintain social distancing. In order to maintain the social distancing must obey the modeling rule (see for example [33]-[40]). Moreover, it is notable that media platforms, through campaigns explaining the importance of social distancing, use of face masks, non-pharmaceutical interventions, hand sanitization, social isolation of the exposed individuals, etc., have a tremendous impact on reducing the virus by spreading awareness all over the world (see for example [41]-[42]).

In this paper, a fractional-order (COVID-19) SITR model is investigated to explain, understand, and forecast the outbreaks of COVID-19 in Saudi Arabia. The proposed model is extended to a system of five first-order ordinary differential equations, three of which have quadratic nonlinearity, with five unknowns, which are the numbers of different groups of people (healthy, infected, ill under 65 years of age, ill over 65 years of age, dead) (see [43]). The model includes nine constant coefficients that explain the effect of various processes such as birth rate, death rate, contact rate, reactivity reduction, and others. The SITR model consists of four compartment: susceptible $\mathbb{S}(t)$, infected $\mathbb{I}(t)$, treatment $\mathbb{T}(t)$, and recovered $\mathbb{R}(t)$. Moreover, the susceptible $\mathbb{S}(t)$ is separated into two parts: $\mathbb{S}_1(t)$ and $\mathbb{S}_2(t)$. The state variables $\mathbb{S}_1(t)$, $\mathbb{S}_2(t)$, $\mathbb{I}(t)$, $\mathbb{T}(t)$ and $\mathbb{R}(t)$ represent, respectively, the densities of people who are yet not infected, the densities of not infected old age or seriously diseased people, the infected people which are infected with this serious disease at the time t, the treatment of this virus, and the recovery of those people who recovered from this

serious disease at time t by using these precautionary measures and it is noticed that a large number of such category exist. The proposed model aims to study the lockdown effect and quarantine probabilities, in controlling the COVID-19 spread in Saudi Arabia. The basic reproduction number R_0 and its impact on the covid-19 pandemic are described. The basic reproduction number R_0 is one of the most crucial quantities in infectious diseases, as R_0 measures how contagious a disease is [39]. The global stability of the infection-free and endemic equilibrium point of the proposed model has been fully established using the Lyapunov-LaSalle type theorem. Some new and important developments for searching for analytical solitary wave solutions and stability analysis for differential equations (see for example [44]-[47]). In this work, a fractional-order (COVID-19) SITR model with nonlinear incidence rate is considered in the sense of Caputo derivative D^{κ}, $0 < \kappa \leq 1$, and is given by

$$\begin{aligned}
D^{\kappa}\mathbb{S}_1(t) &= \Lambda - \beta\mathbb{I}(t)\mathbb{S}_1(t) - \delta\beta\mathbb{T}(t) - \mathbb{S}_1(t),\\
D^{\kappa}\mathbb{S}_2(t) &= \Lambda - \beta\mathbb{I}(t)\mathbb{S}_2(t) - \delta\beta\mathbb{T}(t) - \mathbb{S}_2(t),\\
D^{\kappa}\mathbb{I}(t) &= -\mu\mathbb{I}(t) + \beta\mathbb{I}(t)(\mathbb{S}_1(t) + \mathbb{S}_2(t)) + \delta\beta\mathbb{T}(t) - \alpha\mathbb{I}(t) + \sigma\mathbb{I}(t),\\
D^{\kappa}\mathbb{T}(t) &= \mu\mathbb{I}(t) - \alpha\mathbb{T}(t) - \rho\mathbb{T}(t) + \varepsilon\mathbb{T}(t) + \psi\mathbb{T}(t),\\
D^{\kappa}\mathbb{R}(t) &= -\alpha\mathbb{R}(t) + \rho\mathbb{T}(t),
\end{aligned} \tag{1}$$

with initial data $\mathbb{S}_1(0) = \mathbb{I}_1$, $\mathbb{S}_2(0) = \mathbb{I}_2$, $\mathbb{I}(0) = \mathbb{I}_3$, $\mathbb{T}(0) = \mathbb{I}_4$, and $R(0) = \mathbb{I}_5$. The biological meanings of the parameters in the model (1.1) are existed in Table 1.

Table 1: Parameters description for the novel (COVID-19) SITR model.

Parameters	Description
Λ	the rate of natural birth
β	the rate of contact
δ	the treatment to reduce infection
α	the rate of death
μ	the rate of recovery
σ	the rate of tiredness, dry cough, and fever
ρ	the infection rate of treatment
ε	the rate of sleep
ψ	the rate of healthy food

This paper's contribution is to demonstrate the superiority of fractional order modeling over the integer-order one. The stabilization of the infection is achieved earlier because of the rules of social distancing and confinement. Preventative measures' effectiveness, potential control strategies, and the prediction of future outbreaks were evaluated by using the simplified nonlinear fractional mathematical (COVID-19) SITR model with fractal parameters. The existence of a solution to such a generalized system (1.1) within the desired function's positive range of values is illustrated. The system's stationary points are discussed. We derived an infectious-free equilibrium and endemic-equilibrium points from local and global stability using the reproduction rate. The normalized forward sensitivity index of the basic reproduction number, $\mathcal{R}_0$, is used to perform local sensitivity statistical analysis. Furthermore, simulation findings indicate that increasing preemptive priority has a positive impact. The model is also developed using a numerical algorithm, and the results of a computational experiment are presented. The results of this manuscript may well complement the existing literature as [48]-[54].

2 Properties of Solutions

This section will discuss the solutions' existence, uniqueness, non-negativity, and boundedness. By assuming the following $\Omega = \{(\mathbb{S}_1, \mathbb{S}_2, \mathbb{I}, \mathbb{T}, \mathbb{R}) \in R_+^5 : \mathbb{S}_1 \geq 0, \mathbb{S}_2 \geq 0, \mathbb{I} \geq 0, \mathbb{T} \geq 0, \mathbb{R} \geq 0, \max(|\mathbb{S}_1|, |\mathbb{S}_2|, |\mathbb{I}|, |\mathbb{T}|, |\mathbb{R}|) \leq \eta\}$. Following [49], the existence and uniqueness of the fractional-order model's solutions (1.1) are established in the region $\Omega \times (0, \tau]$.

Theorem 2.1. *If $X_0 = (\mathbb{S}_1(0), \mathbb{S}_2(0), \mathbb{I}(0), \mathbb{T}(0), \mathbb{R}(0)) \in \Omega$ is an initial condition, the solution $X = (\mathbb{S}_1(t), \mathbb{S}_2(t), \mathbb{I}(t), \mathbb{T}(t), \mathbb{R}(t)) \in \Omega$ to the fractional-order model (1.1) is unique, for $t \geq 0$.*

Proof. Suppose that $\Theta(X) = (\Theta_1(X), \Theta_2(X), \Theta_3(X), \Theta_4(X), \Theta_5(X))$ is a mapping with

$$\begin{aligned}
\Theta_1(X) &= \Lambda - \beta \mathbb{I}(t)\mathbb{S}_1(t) - \delta\beta\mathbb{T}(t) - \mathbb{S}_1(t),\\
\Theta_2(X) &= \Lambda - \beta \mathbb{I}(t)\mathbb{S}_2(t) - \delta\beta\mathbb{T}(t) - \mathbb{S}_2(t),\\
\Theta_3(X) &= -\mu\mathbb{I}(t) + \beta\mathbb{I}(t)(\mathbb{S}_1(t) + \mathbb{S}_2(t)) + \delta\beta\mathbb{T}(t) - \alpha\mathbb{I}(t) + \sigma\mathbb{I}(t),\\
\Theta_4(X) &= \mu\mathbb{I}(t) - \alpha\mathbb{T}(t) - \rho\mathbb{T}(t) + \varepsilon\mathbb{T}(t) + \psi\mathbb{T}(t),\\
\Theta_5(X) &= -\alpha\mathbb{R}(t) + \rho\mathbb{T}(t).
\end{aligned}$$

Hence, for $X, \overline{X} \in \Omega$, one obtains

$$\begin{aligned}
\|\Theta(X) - \Theta(\overline{X})\| &= |\Theta_1(X) - \Theta_1(\overline{X})| + |\Theta_2(X) - \Theta_2(\overline{X})| + |\Theta_3(X) - \Theta_3(\overline{X})|\\
&\quad + |\Theta_4(X) - \Theta_4(\overline{X})| + |\Theta_5(X) - \Theta_5(\overline{X})|\\
&\leq (2\eta\beta + 1)|\mathbb{S}_1 - \overline{S}_1| + (2\eta\beta + 1)|\mathbb{S}_2 - \overline{\mathbb{S}}_2| + (4\eta\beta + 2\mu + \sigma + \alpha)|\mathbb{I} - \overline{\mathbb{I}}|\\
&\quad + (3\eta\beta + \alpha + 2\rho + \varepsilon + \psi)|\mathbb{T} - \overline{\mathbb{T}}| + \rho|\mathbb{R} - \overline{\mathbb{R}}|\\
&\leq \Gamma\|X - \overline{X}\|,
\end{aligned} \tag{2}$$

where

$$\Gamma = \max\{2\eta\beta + 1, 4\eta\beta + 2\mu + \sigma + \alpha, 3\eta\beta + \alpha + 2\rho + \varepsilon + \psi, \rho\}.$$

As a result, $\Theta(X)$ satisfies the Lipschitz condition, implying that the fractional-order model (1.1) solution exists and is unique. □

2.1 The Solution's Non-Negativity and Boundedness

Let R_+ be the set of all non-negative real numbers and let $\Omega^+ = \{(\mathbb{S}_1, \mathbb{S}_2, I, T, R) \in R_+^5 : \mathbb{S}_1 \in R_+, \mathbb{S}_2 \in R_+, I \in R_+, T \in R_+, R \in R_+, \Lambda > \beta\delta\mathbb{I}_4\}$.

Theorem 2.2. *The fractional-order model (1.1) has non-negative solutions.*

Proof. One has

$$\begin{aligned}
&D^\kappa \mathbb{S}_1(t)|_{\mathbb{S}_1=0} > 0,\\
&D^\kappa \mathbb{S}_2(t)|_{\mathbb{S}_2=0} > 0,\\
&D^\kappa \mathbb{I}(t)|_{I=0} = \beta\delta\mathbb{I}_4 > 0,\\
&D^\kappa \mathbb{T}(t)|_{T=0} = \mu\mathbb{I}_3 > 0,\\
&D^\kappa \mathbb{R}(t)|_{R=0} = \rho\mathbb{I}_4 > 0.
\end{aligned}$$

Thus, by using Lemmas 5 and 6 in [50], the solutions of the fractional-order model (1.1) are non-negative. □

Theorem 2.3. *The fractional-order model (1.1) has uniformly bounded solutions start in* Ω^+.

Proof. The total population at time t is denoted by

$$\mathbb{N}(t) = \mathbb{S}_1(t) + \mathbb{S}_2(t) + \mathbb{I}(t) + \mathbb{T}(t) + \mathbb{R}(t).$$

By adding the equations in the fractional-order model (1.1) directly, one gets

$$\begin{aligned} D^{\kappa} N(t) &= 2\Lambda - (\mathbb{S}_1 + \mathbb{S}_2 + (\alpha - \sigma)\mathbb{I} + (\alpha + \delta\beta - \epsilon - \psi)\mathbb{T} + \alpha\mathbb{R}) \\ &\leq 2\Lambda - \lambda\mathbb{N}(t), \end{aligned}$$

where $\lambda = \min\{1, \alpha - \sigma, \alpha + \delta\beta - \epsilon - \psi, \alpha\}$. Thus

$$D^{\kappa}\mathbb{N}(t) + \lambda\mathbb{N}(t) \leq 2\Lambda.$$

Following to [51]; Lemma 9, we get

$$0 \leq \mathbb{N}(t) \leq \mathbb{N}(0)\mathbb{E}_{\kappa}(-\lambda t^{\kappa}) + t^{\kappa}\mathbb{E}_{\kappa,\kappa+1}(-\lambda t^{\kappa})),$$

where $\mathbb{E}_{\kappa}$ is the Mittag-Leffler function. Following Lemma 5 and Corollary 6 in [50], one obtains:

$$0 \leq \mathbb{N}(t) \leq \frac{2\Lambda}{\lambda}, \quad t \longrightarrow \infty.$$

Thus, starting in Ω^+, the fractional-order model (1.1) solutions are uniformly bounded in the region

$$Z = \left\{ (\mathbb{S}_1, \mathbb{S}_2, \mathbb{I}, \mathbb{T}, \mathbb{R}) \in \Omega^+ : 0 \leq \mathbb{S}_1 + \mathbb{S}_2 + \mathbb{I} + \mathbb{T} + \mathbb{R} \leq \frac{2\Lambda}{\lambda} \right\}.$$

□

The set Z is obviously positively invariant in the fractional-order model (1.1).

3 Stability Analysis for Equilibriums

In this section, we compute the basic reproduction number $\mathfrak{R}_0$. The local and global asymptotic stability of the infectious-free equilibrium point is also investigated by building appropriate Lyapunov functions. The local and global asymptotic stability of the endemic equilibrium point is also being studied.

3.1 The Reproduction Number

The state variables $(\mathbb{S}_1(t), \mathbb{S}_2(t), \mathbb{I}(t), \mathbb{T}(t), \mathbb{R}(t))$ remain in the biologically meaningful region $\{(\mathbb{S}_1, \mathbb{S}_2, I, T, R) : \mathbb{S}_1 \geq 0, \mathbb{S}_2 \geq 0, I \geq 0, T \geq 0, R \geq 0\}$ is a positively invariant for model (1.1). It's easy to prove that the region Ω is a positively invariant set of the model (1.1).

For $I = 0$, we can easily obtain the infection-free equilibrium $P_0 = \left(\frac{\Lambda}{\alpha}, \frac{\Lambda}{\alpha}, 0, 0, 0\right)$. Let $y = (I, T, R, \mathbb{S}_1, \mathbb{S}_2)^{\mathcal{T}}$, then the fractional-order model (1.1) can be written as

$$y' = \mathcal{F}(y) - \mathcal{Z}(y),$$

where

$$\mathcal{F}(y)=\begin{bmatrix}\beta\mathbb{I}(t)(\mathbb{S}_1(t)+\mathbb{S}_2(t))\\0\\0\\0\\0\end{bmatrix},\quad \mathcal{Z}(y)=\begin{bmatrix}\mu\mathbb{I}(t)-\delta\beta\mathbb{T}(t)+\alpha\mathbb{I}(t)-\sigma\mathbb{I}(t)\\-\mu\mathbb{I}(t)+\alpha\mathbb{T}(t)+\rho\mathbb{T}(t)-\varepsilon\mathbb{T}(t)-\psi\mathbb{T}(t)\\\alpha\mathbb{R}(t)-\rho\mathbb{T}(t)\\-b+\beta\mathbb{I}(t)\mathbb{S}_1(t)+\delta\beta\mathbb{T}(t)+\mathbb{S}_1(t)\\-b+\beta\mathbb{I}(t)\mathbb{S}_2(t)+\delta\beta\mathbb{T}(t)+\mathbb{S}_2(t)\end{bmatrix}.$$

The Jacobian matrices of $\mathcal{F}(y)$ and $\mathcal{Z}(y)$ at P_0 are, respectively,

$$F=\begin{bmatrix}\frac{2\beta\Lambda}{\alpha}&0&0&0&0\\0&0&0&0&0\\0&0&0&0&0\\0&0&0&0&0\\0&0&0&0&0\end{bmatrix},\quad V=\begin{bmatrix}A_{2\times2}&O_{2\times3}\\C_{3\times2}&D_{3\times3}\end{bmatrix},$$

where

$$A_{2\times2}=\begin{bmatrix}\alpha+\mu-\sigma&-\delta\beta\\-\mu&\alpha+\rho-\varepsilon-\psi\end{bmatrix}, D_{3\times3}=\begin{bmatrix}\alpha&0&0\\0&\alpha&0\\0&0&\alpha\end{bmatrix}, C_{3\times2}=\begin{bmatrix}0&-\rho\\\frac{\Lambda\beta}{\alpha}&\delta\beta\\\frac{\Lambda\beta}{\alpha}&\delta\beta\end{bmatrix}.$$

Thus

$$V^{-1}=\begin{bmatrix}A_{2\times2}^{-1}&O_{2\times3}\\\mathbb{E}_{3\times2}&D_{3\times3}^{-1}\end{bmatrix}, \mathbb{E}_{3\times2}=-D_{3\times3}^{-1}C_{3\times2}A_{2\times2}^{-1}.$$

That is

$$V^{-1}=\begin{bmatrix}\frac{\alpha+\rho-\varepsilon-\psi}{(\alpha+\rho-\varepsilon-\psi)(\alpha+\mu-\sigma)-\delta\beta\mu}&\frac{\delta\beta}{(\alpha+\rho-\varepsilon-\psi)(\alpha+\mu-\sigma)-\delta\beta\mu}&0&0&0\\\frac{\mu}{(\alpha+\rho-\varepsilon-\psi)(\alpha+\mu-\sigma)-\delta\beta\mu}&\frac{\alpha+\mu-\sigma}{(\alpha+\rho-\varepsilon-\psi)(\alpha+\mu-\sigma)-\delta\beta\mu}&0&0&0\\\frac{\mu}{(\alpha+\rho-\varepsilon-\psi)(\alpha+\mu-\sigma)-\delta\beta\mu}&\frac{\alpha+\mu-\sigma}{(\alpha+\rho-\varepsilon-\psi)(\alpha+\mu-\sigma)-\delta\beta\mu}&\alpha^3&0&0\\\frac{\rho\mu\alpha^3\beta^2}{(\alpha+\rho-\varepsilon-\psi)(\alpha+\mu-\sigma)-\delta\beta\mu}&\frac{\rho\alpha^3\beta^2(\alpha+\mu-\sigma)}{(\alpha+\rho-\varepsilon-\psi)(\alpha+\mu-\sigma)-\delta\beta\mu}&0&\alpha^3&0\\\frac{\rho\mu\alpha^3\beta^2}{(\alpha+\rho-\varepsilon-\psi)(\alpha+\mu-\sigma)-\delta\beta\mu}&\frac{\rho\alpha^3\beta^2(\alpha+\mu-\sigma)}{(\alpha+\rho-\varepsilon-\psi)(\alpha+\mu-\sigma)-\delta\beta\mu}&0&0&\alpha^3\end{bmatrix}.$$

The spectral radius of the matrix $F.V^{-1}$ can be calculated as follows:

$$\rho(F.V^{-1})=\frac{\delta\beta\mu}{(\alpha+\rho-\varepsilon-\psi)(\alpha+\mu-\sigma-\frac{2\Lambda\beta}{\alpha})}.$$

The fractional-order model's basic reproduction number $\mathfrak{R}_0$ is then

$$\mathfrak{R}_0=\frac{\delta\beta\mu}{(\alpha+\rho-\varepsilon-\psi)\left(\alpha+\mu-\sigma-\frac{2\Lambda\beta}{\alpha}\right)}. \tag{3}$$

3.2 Infectious-Free Equilibrium and Its Stability

Lemma 3.1. *The infection-free equilibrium* $P_0=\left(\frac{\Lambda}{\alpha},\frac{\Lambda}{\alpha},0,0,0\right)$ *is locally asymptotically stable in* Ω *if* $\mathfrak{R}_0<1$ *and unstable if* $\mathfrak{R}_0>1$.

Proof. For the fractional-order model (1.1) at P_0, the Jacobian matrix $J(P_0)$ is given by

$$J(P_0)=\begin{bmatrix}-\alpha&0&\frac{-\Lambda\beta}{\alpha}&-\delta\beta&0\\0&-\alpha&\frac{-\Lambda\beta}{\alpha}&-\delta\beta&0\\0&0&-\alpha-\mu+\sigma+\frac{2\Lambda\beta}{\alpha}&\delta\beta&0\\0&0&\mu&-\alpha-\rho+\varepsilon+\psi&0\\0&0&0&\rho&-\alpha\end{bmatrix},$$

and its characteristic equation is given by

$$\begin{aligned}(\lambda+\alpha)(\lambda+\alpha)(\lambda+\alpha)[\lambda^2+(\alpha+\rho-\varepsilon-\psi+\alpha+\mu-\sigma-\frac{2\Lambda\beta}{\alpha})\lambda \\ +(\alpha+\rho-\varepsilon-\psi)(\alpha+\mu-\sigma-\frac{2\Lambda\beta}{\alpha})-\delta\beta\mu]=0.\end{aligned} \tag{4}$$

From Eq. (3.2), the characteristic values are $\lambda_1=\lambda_2=\lambda_3=-\alpha$, and the other can obtains from the equation

$$\lambda^2+(\alpha+\rho-\varepsilon-\psi+\alpha+\mu-\sigma-\frac{2\Lambda\beta}{\alpha})\lambda+\Big(\alpha+\rho-\varepsilon-\psi\Big)\Big(\alpha+\mu-\sigma-\frac{2\Lambda\beta}{\alpha}\Big)-\delta\beta\mu=0. \tag{5}$$

The infection-free equilibrium point P_0 is stable according to Routh-Hurwits criteria, if and only if all of the characteristic values are <0 [52]. Obviously, λ_1, λ_2, λ_3, are negative. Thus, the stability of Eq. (3.3) relies on whether $\lambda_4<0$, $\lambda_5<0$. The sufficient condition of stability is given by a direct computation of λ_4, λ_5. Thus, from (3.1), the condition that the system (1.1) is locally asymptotically stable at P_0 is $\mathfrak{R}_0<1$. However, the system (1.1) is unstable if $\mathfrak{R}_0>1$. Thus the proof follows. □

Lemma 3.2. *The infection-free equilibrium point P_0 is globally asymptotically stable in Ω if $\mathfrak{R}_0<1$ and unstable if $\mathfrak{R}_0>1$.*

Proof. To show this result, one constructs a suitable Lyapunov function L_1 as follows:

$$L_1=\mu I+\left(\alpha+\mu-\sigma-\frac{2\Lambda\beta}{\alpha}\right)T.$$

With respect to t, the fractional derivative of L_1 is

$$\begin{aligned}D^{\kappa}L_1&=\mu D^{\kappa}I+\left(\alpha+\mu-\sigma-\frac{2\Lambda\beta}{\alpha}\right)D^{\kappa}T\\&=\mu\left[\beta(\mathbb{S}_1+\mathbb{S}_2)-\frac{2\Lambda\beta}{\alpha}\right]I+\left[\delta\beta\mu-(\alpha+\rho-\varepsilon-\psi)\left(\alpha+\mu-\sigma-\frac{2\Lambda\beta}{\alpha}\right)\right]T\\&\leq\left[\delta\beta\mu-(\alpha+\rho-\varepsilon-\psi)\left(\alpha+\mu-\sigma-\frac{2\Lambda\beta}{\alpha}\right)\right]T.\end{aligned}$$

Hence, if $\mathfrak{R}_0<1$, then $D^{\kappa}L_1\leq 0$. Moreover, the largest invariant set of $\{(\mathbb{S}_1,\mathbb{S}_2,\mathbb{I},\mathbb{T},\mathbb{R})\in\Omega: D^{\kappa}L_1=0\}$ is the singleton $\{P_0\}$. Thus, P_0 is globally asymptotically stable by using LaSalle's invariance principle [53]. □

3.3 The Stability of Endemic-Equilibrium Point

To obtain the stability of the endemic-equilibrium point, one assumes that

$$D^{\kappa}\mathbb{S}_1(t)=0,\quad D^{\kappa}\mathbb{S}_2(t)=0,\quad D^{\kappa}\mathbb{I}(t)=0,\quad D^{\kappa}\mathbb{T}(t)=0,\quad D^{\kappa}\mathbb{R}(t)=0.$$

The unique endemic-equilibrium point for $\mathbb{I}^* > 0$ is $P^* = (\mathbb{S}_1^*, \mathbb{S}_2^*, \mathbb{I}^*, \mathbb{T}^*, \mathbb{R}^*)$, where

$$\begin{aligned}
\mathbb{S}_1^* &= \frac{1}{2\beta\Re_0(\alpha+\rho-\varepsilon-\psi)} + \frac{\Lambda}{\alpha},\\
\mathbb{S}_2^* &= S_1^*,\\
\mathbb{I}^* &= \frac{(\alpha+\rho-\varepsilon-\psi)(\Lambda-\alpha S_1^*)}{S_1^*\beta(\alpha+\rho-\varepsilon-\psi)+\delta\beta\mu},\\
\mathbb{T}^* &= \frac{\Lambda\mu-\alpha\mu S_1^*}{S_1^*\beta(\alpha+\rho-\varepsilon-\psi)+\delta\beta\mu},\\
\mathbb{R}^* &= \frac{\Lambda\mu\rho-\rho\alpha\mu S_1^*}{S_1^*\alpha\beta(\alpha+\rho-\varepsilon-\psi)+\delta\beta\mu\alpha}.
\end{aligned}$$

Lemma 3.3. *In Ω, the endemic equilibrium point P^* is asymptotically stable locally.*

Proof. The Jacobian matrix $J(P^*)$ of the fractional order system (1.1) is given by the matrix

$$J(P^*) = \begin{bmatrix}
-\beta\mathbb{I}^*-\alpha & 0 & -\beta\mathbb{S}_1^* & -\delta\beta & 0\\
0 & -\beta\mathbb{I}^*-\alpha & -\beta\mathbb{S}_2^* & -\delta\beta & 0\\
\beta\mathbb{I}^* & \beta\mathbb{I}^* & -\alpha-\mu+\sigma+\beta\mathbb{S}_1^*+\beta\mathbb{S}_2^* & \delta\beta & 0\\
0 & 0 & \mu & -\alpha-\rho+\varepsilon+\psi & 0\\
0 & 0 & 0 & \rho & -\alpha
\end{bmatrix},$$

and its characteristic equation is given by

$$(\lambda+\alpha)(\lambda+\beta\mathbb{I}+\alpha)(a_1\lambda^3+a_2\lambda^2+a_3\lambda+a_4)=0, \tag{6}$$

where

$$\begin{aligned}
\ell_1 &= 1,\\
\ell_2 &= 3\alpha+\mu+\rho-\varepsilon-\psi-\sigma+\beta(\mathbb{I}^*-\mathbb{S}_1^*-\mathbb{S}_2^*),\\
\ell_3 &= (\beta\mathbb{I}^*+\alpha)(\alpha+\mu-\sigma-\beta(\mathbb{S}_1^*+S_2^*))+\beta^2\mathbb{I}^*(\mathbb{S}_2^*-\mathbb{S}_1^*)-\delta\beta\mu\\
&\quad+(\alpha+\rho-\varepsilon-\psi)\left(2\alpha+\mu-\sigma-\beta(\mathbb{I}^*-\mathbb{S}_1^*-\mathbb{S}_2^*)\right),\\
\ell_4 &= (\beta\mathbb{I}^*+\alpha)(\alpha+\mu-\sigma-\beta(\mathbb{S}_1^*+\mathbb{S}_2^*))\,(\alpha+\rho-\varepsilon-\psi)\\
&\quad+\beta^2\mathbb{I}^*(\mathbb{S}_2^*-\mathbb{S}_1^*)\,(\alpha+\rho-\varepsilon-\psi)-\delta\beta\mu(\beta\mathbb{I}^*+\alpha).
\end{aligned}$$

From Eq. (3.4), the characteristic values are given by: $\lambda_1 = -\alpha, \lambda_2 = -\beta\mathbb{I}^*-\alpha$, and the other values can be obtained from the equation

$$\ell_1\lambda^3+\ell_2\lambda^2+\ell_3\lambda+\ell_4=0.$$

Based on Routh-Hurwitz conditions [52], the Routh-Hurwitz array for the Jacobian matrix $J(P^*)$ is as follows:

$$D_1(P^*) = -\begin{vmatrix}
\ell_1 & \ell_2\\
\ell_2 & \ell_4\\
\frac{(\ell_2\ell_3-\ell_4\ell_1)}{\ell_2} & 0\\
\ell_4 & 0
\end{vmatrix}.$$

Verifying that $\frac{(\ell_2\ell_3-\ell_4\ell_1)}{\ell_2}$ has the same sign with ℓ_3, the other three eigenvalues λ_3, λ_4, λ_5 will then have negative real parts. Since ℓ_1, ℓ_2, ℓ_3, ℓ_4, $\frac{(\ell_2\ell_3-\ell_4\ell_1)}{\ell_2}$ are all positive and $\ell_2\ell_3 > \ell_4\ell_1$ hold, the conditions of stability of Routh-Hurwitz are thus fulfilled. Thus, the endemic-equilibrium point P^* is locally asymptotically stable. □

Lemma 3.4 ([21]). Let $\theta(t) \in R^+$ be a continuous differentiable function. Thus, for any time instant $t \geq t_0$,

$$D^{\kappa}\left(\theta(t) - \theta^* - \theta^* \ln \frac{\theta(t)}{\theta^*}\right) \leq \left(1 - \frac{\theta^*}{\theta(t)}\right) D^{\kappa}\theta(t), \quad \theta^* \in R^+.$$

Lemma 3.5. *Under the condition $\mathfrak{R}_0 > 1$, the endemic equilibrium point P^* is globally asymptotically stable if $\frac{\mathbb{S}_1}{\mathbb{S}_1^*} > \frac{\mathbb{S}_2}{\mathbb{S}_2^*} > \frac{\mathbb{T}}{\mathbb{T}^*} > \frac{\mathbb{I}^*}{\mathbb{I}} > 1$, and $\mu + \alpha > \sigma + \beta(\mathbb{S}_1^* + \mathbb{S}_2^*)$.*

Proof. The model (1.1) has unique positive equilibrium P^* if $\mathfrak{R}_0 > 1$ holds. Then we consider $L_2 : \Omega \longrightarrow R$ as the following Lyapunov function:

$$L_2(\mathbb{S}_1, \mathbb{S}_2, \mathbb{I}) = \left(\mathbb{S}_1 - \mathbb{S}_1^* - \mathbb{S}_1^* \ln \frac{\mathbb{S}_1}{\mathbb{S}_1^*}\right) + \left(\mathbb{S}_2 - \mathbb{S}_2^* - \mathbb{S}_2^* \ln \frac{\mathbb{S}_2}{\mathbb{S}_2^*}\right) + \left(\mathbb{I} - \mathbb{I}^* - \mathbb{I}^* \ln \frac{\mathbb{I}^*}{\mathbb{I}}\right).$$

From Lemma 4, with respect to t, one obtains the fractional derivative of L_2 as

$$\begin{aligned}
D^{\kappa}L_2(\mathbb{S}_1, \mathbb{S}_2, \mathbb{I}) &\leq \left(\frac{\mathbb{S}_1 - \mathbb{S}_1^*}{\mathbb{S}_1}\right) D^{\kappa}\mathbb{S}_1 + \left(\frac{\mathbb{S}_2 - \mathbb{S}_2^*}{\mathbb{S}_2}\right) D^{\kappa}\mathbb{S}_2 + \left(\frac{\mathbb{I} - \mathbb{I}^*}{\mathbb{I}}\right) D^{\kappa}\mathbb{I} \\
&= \left(\frac{\mathbb{S}_1 - \mathbb{S}_1^*}{\mathbb{S}_1}\right)(\Lambda - \beta\mathbb{I}\mathbb{S}_1 - \delta\beta\mathbb{T} - \mathbb{S}_1) + \left(\frac{\mathbb{S}_2 - \mathbb{S}_2^*}{\mathbb{S}_2}\right)(\Lambda - \beta I\mathbb{S}_2 - \delta\beta\mathbb{T} - \mathbb{S}_2) \\
&+ \left(\frac{\mathbb{I} - \mathbb{I}^*}{\mathbb{I}}\right)(-\mu\mathbb{I} + \beta\mathbb{I}(\mathbb{S}_1 + \mathbb{S}_2) + \delta\beta\mathbb{T} - \alpha\mathbb{I} + \sigma\mathbb{I}) \\
&= \left(\frac{\mathbb{S}_1 - \mathbb{S}_1^*}{\mathbb{S}_1}\right)(-\beta(\mathbb{I}\mathbb{S}_1 - \mathbb{I}^*\mathbb{S}_1^*) - \delta\beta(\mathbb{T} - \mathbb{T}^*) - (\mathbb{S}_1 - \mathbb{S}_1^*)) \\
&+ \left(\frac{\mathbb{S}_2 - \mathbb{S}_2^*}{\mathbb{S}_2}\right)(-\beta(\mathbb{I}\mathbb{S}_2 - \mathbb{I}^*\mathbb{S}_2^*) - \delta\beta(\mathbb{T} - \mathbb{T}^*) - (\mathbb{S}_2 - \mathbb{S}_2^*)) \\
&+ \left(\frac{\mathbb{I} - \mathbb{I}^*}{I}\right)(-(\mu + \alpha - \sigma)(\mathbb{I} - \mathbb{I}^*) + \beta\mathbb{I}(\mathbb{S}_1 + \mathbb{S}_2) - \beta\mathbb{I}^*(\mathbb{S}_1^* + \mathbb{S}_2^*) + \delta\beta(\mathbb{T} - \mathbb{T}^*)) \\
&\leq -\beta\mathbb{I}^*\frac{(\mathbb{S}_1 - \mathbb{S}_1^*)^2}{\mathbb{S}_1} - \beta\mathbb{I}\frac{(\mathbb{S}_2 - \mathbb{S}_2^*)^2}{\mathbb{S}_2} - (\mu + \alpha - \sigma - (\mathbb{S}_1^* + \mathbb{S}_2^*)\beta)\frac{(\mathbb{I} - \mathbb{I}^*)^2}{\mathbb{I}} \\
&- \beta\Big(\frac{(\mathbb{S}_1 - \mathbb{S}_1^*)^2}{\mathbb{S}_1} + \frac{(\mathbb{S}_2 - \mathbb{S}_2^*)^2}{\mathbb{S}_2}\Big)(\mathbb{I}^* - \mathbb{I}) + \frac{\beta\delta}{\mathbb{S}_1}(\mathbb{S}_1 - \mathbb{S}_1^*)(\mathbb{T}^* - \mathbb{T}) \\
&+ \frac{\beta\delta}{\mathbb{S}_2}(\mathbb{S}_2 - \mathbb{S}_2^*)(\mathbb{T}^* - \mathbb{T}) + \frac{\beta\delta}{\mathbb{I}}(\mathbb{I} - \mathbb{I}^*)(\mathbb{T} - \mathbb{T}^*).
\end{aligned}$$

Thus, $D^{\kappa}L_2(\mathbb{S}_1, \mathbb{S}_2, \mathbb{I}) < 0$ in V. Furthermore $D^{\kappa}L_2(\mathbb{S}_1, \mathbb{S}_2, \mathbb{I}) = 0$ implies that $\mathbb{S}_1 = \mathbb{S}_1^*$, $\mathbb{S}_2 = \mathbb{S}_2^*$, and $\mathbb{I} = \mathbb{I}^*$. Therefore, the singleton $\{P^*\}$ is the only invariant set such that $D^{\kappa}L_2(\mathbb{S}_1, \mathbb{S}_2, \mathbb{I}) = 0$. The Lasalle invariance principle (see [55], [19]) gives conclusion that P^* is globally asymptotically stable. □

4 Statistical Analysis

Sensitivity statistical analysis is used to evaluate the relative influence of several factors on a model's stability when data is unknown. The analysis can also determine which parameters are crucial. Using both local and global techniques, one can calculate the sensitivity indices of the basic reproduction number, $\mathfrak{R}_0$, with respect to the parameters of the model.

4.1 Local Sensitivity Statistical Analysis

In local sensitivity analysis, the normalized forward sensitivity index is utilized. With respect to the parameters in our model, the sensitivity index of $\mathfrak{R}_0$ is computed as follows:

$$\Gamma_{\upsilon}^{\mathfrak{R}_0} = \frac{\partial \mathfrak{R}_0}{\partial \upsilon} \times \frac{\upsilon}{\mathfrak{R}_0},$$

where υ is a value from Table 2, and $\mathfrak{R}_0$ is derived by using Eq (3.1). By substituting the parameter values into Eq (3.1), the sensitivity indices of $\mathfrak{R}_0$ computed with Maple are listed in Table 2. Thus, one obtains

$$\begin{aligned}
\frac{\partial \mathfrak{R}_0}{\partial \Lambda} &= \frac{2\delta\beta^2}{\alpha\left(\alpha+\rho-\varepsilon-\psi\right)\left(\alpha+\mu-\sigma-\frac{2\Lambda\beta}{\alpha}\right)^2} > 0,\\
\frac{\partial \mathfrak{R}_0}{\partial \beta} &= \frac{\delta\mu\left(\alpha+\mu-\sigma-\frac{2\Lambda\beta}{\alpha}\right)-\left(\delta\beta\mu\right)\left(-\frac{2\Lambda}{\alpha}\right)}{\left(\alpha+\rho-\varepsilon-\psi\right)\left(\alpha+\mu-\sigma-\frac{2\Lambda\beta}{\alpha}\right)^2} > 0,\\
\frac{\partial \mathfrak{R}_0}{\partial \delta} &= \frac{\beta\mu}{\left(\alpha+\rho-\varepsilon-\psi\right)\left(\alpha+\mu-\sigma-\frac{2\Lambda\beta}{\alpha}\right)} < 0,\\
\frac{\partial \mathfrak{R}_0}{\partial \alpha} &= \frac{-\delta\beta\mu\left[\left(\alpha+\mu-\sigma-\frac{2\Lambda\beta}{\alpha}\right)+\left(\alpha+\rho-\varepsilon-\psi\right)\left(1+\frac{2\Lambda\beta}{\alpha^2}\right)\right]}{\left(\alpha+\rho-\varepsilon-\psi\right)^2\left(\alpha+\mu-\sigma-\frac{2\Lambda\beta}{\alpha}\right)^2} < 0,\\
\frac{\partial \mathfrak{R}_0}{\partial \mu} &= \frac{\delta\beta\left(\alpha-\sigma-\frac{2\Lambda\beta}{\alpha}\right)}{\left(\alpha+\rho-\varepsilon-\psi\right)\left(\alpha+\mu-\sigma-\frac{2\Lambda\beta}{\alpha}\right)^2} < 0,\\
\frac{\partial \mathfrak{R}_0}{\partial \sigma} &= \frac{\delta\beta\mu}{\left(\alpha+\rho-\varepsilon-\psi\right)\left(\alpha+\mu-\sigma-\frac{2\Lambda\beta}{\alpha}\right)^2} > 0,\\
\frac{\partial \mathfrak{R}_0}{\partial \rho} &= \frac{-\delta\beta\mu}{\left(\alpha+\rho-\varepsilon-\psi\right)^2\left(\alpha+\mu-\sigma-\frac{2\Lambda\beta}{\alpha}\right)} > 0,\\
\frac{\partial \mathfrak{R}_0}{\partial \epsilon} &= \frac{\delta\beta\mu}{\left(\alpha+\rho-\varepsilon-\psi\right)^2\left(\alpha+\mu-\sigma-\frac{2\Lambda\beta}{\alpha}\right)} < 0,\\
\frac{\partial \mathfrak{R}_0}{\partial \psi} &= \frac{\delta\beta\mu}{\left(\alpha+\rho-\varepsilon-\psi\right)^2\left(\alpha+\mu-\sigma-\frac{2\Lambda\beta}{\alpha}\right)} < 0.
\end{aligned} \tag{7}$$

By substituting the parameter values into Eq (4.1), we can determine the sensitivity of $\mathfrak{R}_0$ as follows:

$$\begin{aligned}
\Gamma_{\Lambda}^{\mathfrak{R}_0} &= \frac{\partial \mathfrak{R}_0}{\partial \Lambda} \times \frac{\Lambda}{\mathfrak{R}_0} = -18.6, & \Gamma_{\rho}^{\mathfrak{R}_0} &= \frac{\partial \mathfrak{R}_0}{\partial \rho} \times \frac{\rho}{\mathfrak{R}_0} = -1.2,\\
\Gamma_{\sigma}^{\mathfrak{R}_0} &= \frac{\partial \mathfrak{R}_0}{\partial \sigma} \times \frac{\sigma}{\mathfrak{R}_0} = -0.11, & \Gamma_{\beta}^{\mathfrak{R}_0} &= \frac{\partial \mathfrak{R}_0}{\partial \beta} \times \frac{\beta}{\mathfrak{R}_0} = -0.0094,\\
\Gamma_{\delta}^{\mathfrak{R}_0} &= \frac{\partial \mathfrak{R}_0}{\partial \delta} \times \frac{\delta}{\mathfrak{R}_0} = 0.18, & \Gamma_{\varepsilon}^{\mathfrak{R}_0} &= \frac{\partial \mathfrak{R}_0}{\partial \varepsilon} \times \frac{\varepsilon}{\mathfrak{R}_0} = 0.40,\\
\Gamma_{\mu}^{\mathfrak{R}_0} &= \frac{\partial \mathfrak{R}_0}{\partial \mu} \times \frac{\mu}{\mathfrak{R}_0} = 0.59, & \Gamma_{\psi}^{\mathfrak{R}_0} &= \frac{\partial \mathfrak{R}_0}{\partial \psi} \times \frac{\psi}{\mathfrak{R}_0} = 0.80,\\
\Gamma_{\alpha}^{\mathfrak{R}_0} &= \frac{\partial \mathfrak{R}_0}{\partial \alpha} \times \frac{\alpha}{\mathfrak{R}_0} = 4.2.
\end{aligned} \tag{8}$$

Thus, one obtains

Table 2: Parameters description for the novel (COVID-19) SITR model.

Parameters	Description	Sensitivity Index
Λ	0.3	-18.6
ρ	0.3	-1.2
σ	0.005	-0.11
β	0.35	-0.0094
δ	0.3	0.18
ε	0.1	0.40
μ	0.55	0.59
ψ	0.2	0.80
α	0.25	4.2

4.2 Dynamics of $(\mathbb{S}_1 - \mathbb{S}_2 - \mathbb{I} - \mathbb{T} - \mathbb{R})$

In this subsection, we illustrate the dynamics of $\mathbb{S}_1(t)$, $\mathbb{S}_2(t)$, $\mathbb{I}(t)$, $\mathbb{T}(t)$, and $\mathbb{R}(t)$ for different values of κ when $\mathfrak{R}_0 = 1.5024$.

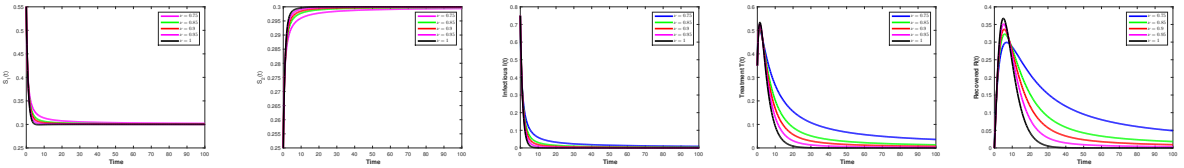

(a) (b) (c) (d) (e)

Figure 1: Dynamics of $\mathbb{S}_1(t)$, $\mathbb{S}_2(t)$, $\mathbb{I}(t)$, $\mathbb{T}(t)$, and $\mathbb{R}(t)$ for different values of κ when $\mathfrak{R}_0 = 0.4190$.

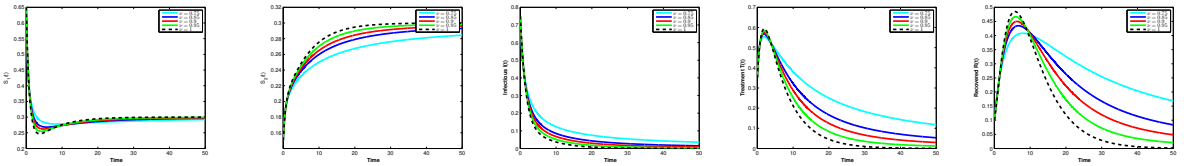

(a) (b) (c) (d) (e)

Figure 2: Dynamics of $\mathbb{S}_1(t)$, $\mathbb{S}_2(t)$, $\mathbb{I}(t)$, $\mathbb{T}(t)$, and $\mathbb{R}(t)$ for different values of κ when $\mathfrak{R}_0 = 1.5024$.

4.3 Contact Rate β

We study the effects of the β contact rate in the COVID-19 spread dynamics. The effects of different contact rates on the downward modulation of this virus are illustrated in Figures 3 to 10. As illustrated in Fig. 3 (c), Fig. 5 (c), Fig. 7 (c), and Fig. 9 (c), a reduced contact rate, analogous to the effects of fractional order, significantly delays the peak and reduces the number of infected cases (c). The effect of contact rate on the dynamics is significant for the other fractional orders, as seen in Figs. 5-7. In infected cases, reducing contact parameters leads to a significant decrease, where decreasing contact rates while keeping other parameters constant maintains $\mathfrak{R}_0$ below 1.

Vaccines are still recommended to minimize the rate of Cov-19 contact and spread. It should be noted that by using the smaller fractional order κ to control the transmission rate will result in a substantial reduction in the infected cases.

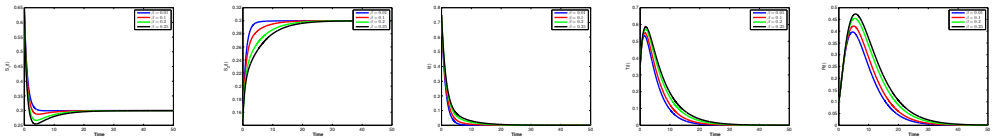

(a) (b) (c) (d) (e)

Figure 3: Solution profiles for $\mathbb{S}_1(t)$, $\mathbb{S}_2(t)$, $\mathbb{I}(t)$, $\mathbb{T}(t)$, and $\mathbb{R}(t)$ with different β when $\kappa = 1$ and $\mathfrak{R}_0 = 0.4190$.

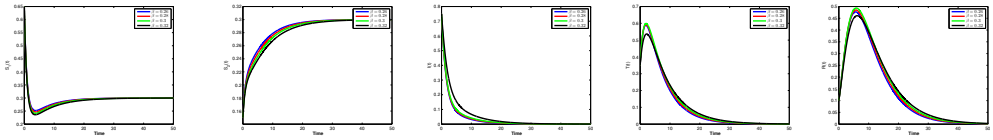

(a) (b) (c) (d) (e)

Figure 4: Solution profiles for $\mathbb{S}_1(t)$, $\mathbb{S}_2(t)$, $\mathbb{I}(t)$, $\mathbb{T}(t)$, and $\mathbb{R}(t)$ with different β when $\kappa = 1$ and $\mathfrak{R}_0 = 1.5024$.

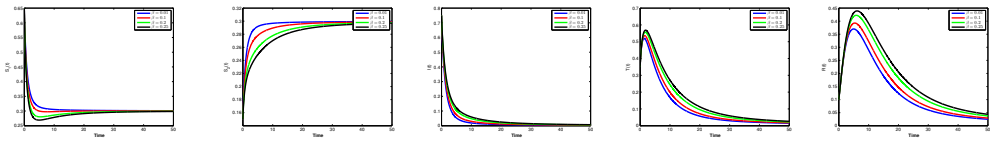

(a) (b) (c) (d) (e)

Figure 5: Solution profiles for $\mathbb{S}_1(t)$, $\mathbb{S}_2(t)$, $\mathbb{I}(t)$, $\mathbb{T}(t)$, and $\mathbb{R}(t)$ with different β when $\kappa = 0.9$ and $\mathfrak{R}_0 = 0.4190$.

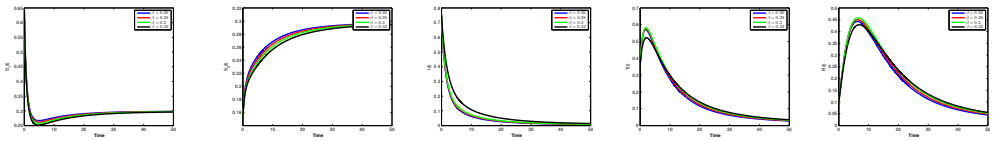

(a) (b) (c) (d) (e)

Figure 6: Solution profiles for $\mathbb{S}_1(t)$, $\mathbb{S}_2(t)$, $\mathbb{I}(t)$, $\mathbb{T}(t)$, and $\mathbb{R}(t)$ with different β when $\kappa = 0.9$ and $\mathfrak{R}_0 = 1.5024$.

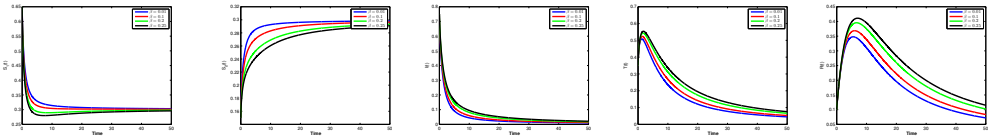

(a) (b) (c) (d) (e)

Figure 7: Solution profiles for $\mathbb{S}_1(t)$, $\mathbb{S}_2(t)$, $\mathbb{I}(t)$, $\mathbb{T}(t)$, and $\mathbb{R}(t)$ with different β when $\kappa = 0.8$ and $\mathfrak{R}_0 = 0.4190$.

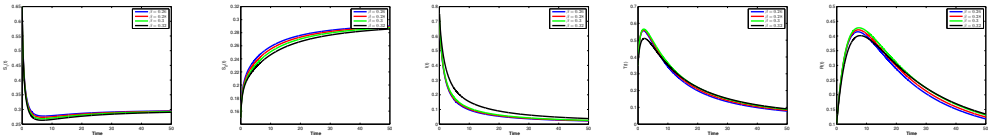

(a) (b) (c) (d) (e)

Figure 8: Solution profiles for $\mathbb{S}_1(t)$, $\mathbb{S}_2(t)$, $\mathbb{I}(t)$, $\mathbb{T}(t)$, and $\mathbb{R}(t)$ with different β when $\kappa = 0.8$ and $\mathfrak{R}_0 = 1.5024$.

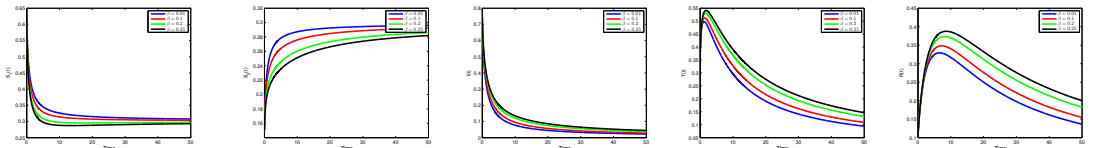

(a) (b) (c) (d) (e)

Figure 9: Solution profiles for $\mathbb{S}_1(t)$, $\mathbb{S}_2(t)$, $\mathbb{I}(t)$, $\mathbb{T}(t)$, and $\mathbb{R}(t)$ with different β when $\kappa = 0.7$ and $\mathfrak{R}_0 = 0.4190$.

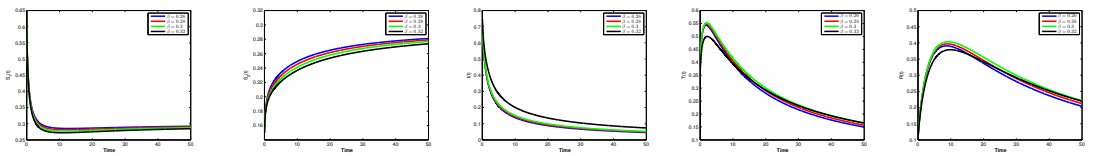

(a) (b) (c) (d) (e)

Figure 10: Solution profiles for $\mathbb{S}_1(t)$, $\mathbb{S}_2(t)$, $\mathbb{I}(t)$, $\mathbb{T}(t)$, and $\mathbb{R}(t)$ with different β when $\kappa = 0.7$ and $\mathfrak{R}_0 = 1.5024$.

4.4 Phase Plot ($\mathbb{S}_1 - \mathbb{S}_2 - \mathbb{I} - \mathbb{T} - \mathbb{R}$)

The absence of infection outbreaks and a noticeable decrease in infectious waves were seen in our findings. Fig. 11 shows the simulation output of the COVID-19 model for $\mathfrak{R}_0 = 0.4190 < 1$. Lastly, the step plots for $\mathbb{S}_1 - \mathbb{S}_2 - \mathbb{I} - \mathbb{T} - \mathbb{R}$ states are shown in Figs. 11 and 12, respectively, supporting local stability for $\mathfrak{R}_0 = 1.5024$. Numerical simulation of the epidemic model of fractional order (1.1), when $\beta = 0.26$ and $\mathfrak{R}_0 = 1.5024 > 1$ (each infected individual infects more than one other population member and spreads a self-sustaining group of infectious individuals), with Table 2 parameter values.

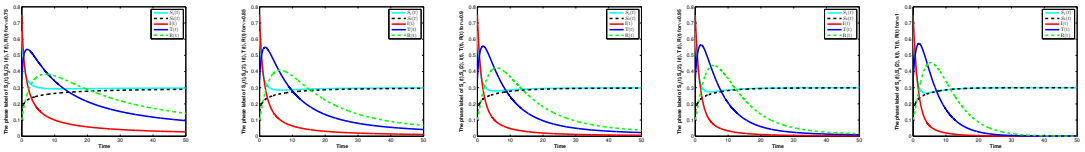

(a) $\kappa = 0.75$ (b) $\kappa = 0.85$ (c) $\kappa = 0.9$ (d) $\kappa = 0.95$ (e) $\kappa = 0.1$

Figure 11: Phase plot $(\mathbb{S}_1 - \mathbb{S}_2 - \mathbb{I} - \mathbb{T} - \mathbb{R})$ for $\mathfrak{R}_0 = 0.4190$.

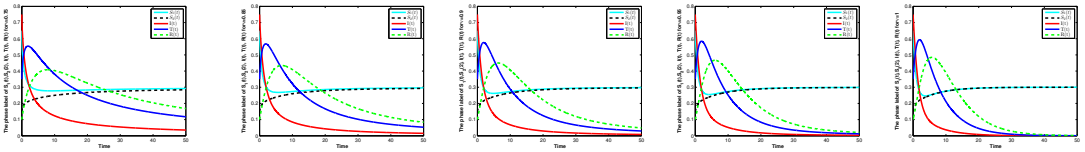

(a) $\kappa = 0.75$ (b) $\kappa = 0.85$ (d) $\kappa = 0.95$ (e) $\kappa = 0.1$

(e) $\kappa = 0.9$

Figure 12: Phase plot $(\mathbb{S}_1 - \mathbb{S}_2 - \mathbb{I} - \mathbb{T} - \mathbb{R})$ for $\mathfrak{R}_0 = 1.5024$.

5 Discussion of Results

Numerical simulations of the proposed time-fractional order COVID-19 system are presented in investigating the spread and containment strategies of coronavirus infection. Several intrinsic aspects of the COVID-19 model that could be detected in time using the fractional derivative $(0 < \kappa < 1)$ as compared to the classical order $\kappa = 1$ are of interest. The numerical COVID-19 model proposed for different fractional-order values κ is simulated using a set of reasonable parameter values in Table 1 to support analytical results and numerically evaluate control strategy effectiveness. When $\beta = 0.2$ (hence $\mathfrak{R}_0 = 0.4190 < 1$), Fig. 1 shows the global stability of the model's infection-free equilibrium (1.1) under potentially different conditions. As predicted, the solutions of (1.1) converge to a single disease-free equilibrium $P_0 = (1.2000, 1.2000, 0, 0, 0)$. As a result, P_0 is globally asymptotically stable for the system (1.1).

Fractional orders have distinct effects; the solution curves for $0 < \kappa < 1$ show a delay at the epidemic peak and flatten out faster, as shown in Fig. 1 (c), (d), and (e). The effect of κ is substantially more pronounced for smaller orders; for example, compare $\kappa = 0.9$ and $\kappa = 0.6$ in Fig. 1 (d), (e). Although the number of infected individuals has decreased for smaller fractional orders, the number of people who are susceptible has increased (see Fig. 1(a)). Figures 2 shows the global stabilities of the endemic model equilibrium (1.1) under potentially various situations when $\beta = 0.28$ (such that $\mathfrak{R}_0 = 1.5024 > 1$). The other parameter values are listed in Table 1. As predicted, the solutions of (1.1) converge to the unique endemic equilibrium of P^*. According to Lemma 5, $P^* = (0.7090, 0.7090, 0.3202, 0.7044, 2.8176)$, is globally asymptotically stable. Fractional orders have significant consequences; the solution trajectories for $0 < \kappa < 1$ show a delay at the epidemic peak and flatten off faster, as shown in Fig. (c), (d), and (d) are the second, third, and fourth sentences, respectively (e). The impact of κ is significantly more evident for smaller orders; for example, compare $\kappa = 0.9$ and $\kappa = 0.6$ in Fig. (d) 2 (e). Although the number of infected individuals has decreased significantly for smaller fractional orders, the number of people who are susceptible has increased (see Fig. 2(a)).

One of the great advantages of the Caputo fractional derivative is that it minimizes the number

of susceptible and infected while maximizing the number of recovered population from covid-19 virus. Also, we note that when the $S_1(t)$ decreases, $T(t)$, as well as $R(t)$, get increases. However, at some point, both the $I(t)$ start to decrease. And this gets $R(t)$ increased as seen in Figures 1. 2 (e). This is one of the advantages of fractional order over integer order. Moreover, one can propose appropriate strategies to control and prevent the disease based on that data. According to Theorem 3, one should set the parameters such that $\mathfrak{R}_0 < 1$. This is an effective strategy for controlling and preventing the disease. The sensitivity indices indicated the complexities of variable $\mathfrak{R}_0$ relationship to the model parameters. The positive (negative) index indicates that raising the parameter value leads the value of $\mathfrak{R}_0$ to increase (decrease). Figure 2 displays the sensitivity index of each parameter in model (4.2).

Finally, from the sensitivity indices in Table 2, one can see that when the parameter values δ, ε, μ, ψ, and α increase while the other parameter values stay constant, the value of $\mathcal{R}_0$ increases. This means an increase in the endemic rate of the disease, as the indicators show positive signs. On the other hand, the value of $\mathcal{R}_0$ decreases if the parameter values Λ, ρ, σ, and β are decreased while the rest of the parameter values stay constant. This indicates a decrease in illness endurance because the indicator has a negative sign. Mortality α and healthy eating rate ψ are the most sensitive parameters. The recovery rate μ and sleep rate ε are the other key parameters that are sensitive.

6 Conclusions

The epidemiological-based fractional SITR model and the conditions for infection-free equilibrium asymptotic stability were investigated in this study. The proposed model is extended to a system of five first-order ordinary differential equations, three of which have quadratic nonlinearity, with five unknowns, which are the numbers of different groups of people (healthy, infected, ill under 65 years of age, ill over 65 years of age, dead). The model includes nine constant coefficients that explain the effect of various processes such as birth rate, death rate, contact rate, reactivity reduction, and others. In the sense of four susceptible ($\mathbb{S}$), infected ($\mathbb{I}$), treatment ($\mathbb{T}$), and recovered ($\mathbb{R}$) individuals, the existence and uniqueness of the SITR fractal model, expanded by the Caputo fractional derivative, is established. The basic reproduction number was obtained, which determines whether or not the infection is extinguished. The global stability of the infection-free balance and endemic equilibrium point of the system (1.1) has been fully established using the Lyapunov-LaSalle type theorem. The basic reproduction number $\mathfrak{R}_0$ has been used to control the dynamics of the fractional SITR model completely. The proposed model only has a globally stable infection-free equilibrium if the reproduction number is less than or equal to one, which means that the infection-free equilibrium will eventually die out. This implies that the greater a system's quarantine probabilities, the lower its chances of becoming endemic.

Our model simulations and predictions suggest that the new coronavirus disease may show oscillatory dynamics in the future, but can be controlled by maintaining social distance. Our model predicts that the disease can even be eliminated by isolating populations with coronavirus symptoms under strict hygiene measures and social distances. Our study could also have a significant impact on the size and duration of the epidemic by implementing quarantine programs in a timely manner, avoiding mass rallies, rallies, and social distances, and implementing comprehensive blockade measures.

Future expansions of this study can be applied to other states to provide pandemic predictions. Our future research may also consider applying optimal control theory to provide decision-makers with better strategies for controlling the spread of COVID19. This COVID 19 model can also be

used to study other infectious disease systems.

Acknowledgement This research is a part of a project entitled "Using statistics and mathematical modelling to understand infectious disease outbreaks: A case study of the Covid19 epidemic and its impact on the Al-Baha region". This project was funded by the Deanship of Scientific Research, Albaha University, KSA (Grant No. 1442/21). The assistance of the deanship is gratefully acknowledged.

Conflicts of Interest The authors declare no conflict of interest.

References

[1] N. H. Abel (2012). Solution de quelques problemes a l'aide d'integrales definies. In *L. Sylow & S. Lie (Eds.), Oeuvres Complétes de Niels Henrik Abel: Nouvelle Edition (Cambridge Library Collection - Mathematics,* pp. 11–27. Cambridge University Press, Cambridge, UK. https://doi.org/10.1017/CBO9781139245807.003

[2] R. Capponetto, G. Dongola, L. Fortuna & I. Petras (2010). Fractional order systems: Modelling and control applications. In *World Scientific Series on Nonlinear Science Series A: Volume 72,* pp. 1–32. World Scientific, Singapore.

[3] M. H. Alshehri, F. Z. Duraihem, A. Alalyani & S. Saber (2021). A caputo (discretization) fractional-order model of glucose-insulin interaction: numerical solution and comparisons with experimental data. *Journal of Taibah University for Science,* 15(1), 26–36. https://doi.org/10.1080/16583655.2021.1872197

[4] S. Saber, Azza M. Alghamdi, Ghada A. Ahmed & Khulud M. Alshehri (2022). Mathematical modelling and optimal control of pneumonia disease in sheep and goats in Al-Baha region with cost-effective strategies. *AIMS Mathematics,* 7(7), 12011–12049. https://doi.org/10.3934/math.2022669

[5] Alalyani, Ahmad & S. Saber (2022). Stability analysis and numerical simulations of the fractional COVID-19 pandemic model. *International Journal of Nonlinear Sciences and Numerical Simulation*, 14 pages. https://doi.org/10.1515/ijnsns-2021-0042

[6] A. M. A. El-Sayed, H. M. Nour, A. Elsaid, A. E. Matouk & A. Elsonbaty (2016). Dynamical behaviors, circuit realization, chaos control and synchronization of a new fractional order hyperchaotic system. *Applied Mathematical Modelling,* 40(5-6), 3516–3534. https://doi.org/10.1016/j.apm.2015.10.010

[7] M. A. Dokuyucu & H. Bulut (2020). A fractional order model for Ebola virus with the new Caputo fractional derivative without singular kernel. *Chaos, Solitons & Fractals*, 134, 109717. https://doi.org/10.1016/j.chaos.2020.109717

[8] M. A. Dokuyucu (2020). A fractional order alcoholism model via Caputo Fabrizio derivative. *AIMS Mathematics*, 5(2), 781–797. https://doi.org/10.3934/math.2020053

[9] A. M. A. El-Sayed, El-Mesiry, A.& El-Saka, H. (2007). On the fractional-order logistic equation. *Applied Mathematics Letters,* 20 (7), 817–823. https://doi.org/10.1016/j.aml.2006.08.013

[10] Jia, G. L.& Ming, Y. X. (2006). Study on the viscoelasticity of cancellous bone based on higher-order fractional models. In *2008 2nd International Conference on Bioinformatics and Biomedical Engineering*, pp. 1733–1736. IEEE, Shanghai, China. https://doi.org/10.1109/ICBBE.2008.761

[11] R. Magin (2004). Fractional calculus in bioengineering. *Critical Reviews in Biomedical Engineering*, 32(1), 13–77. https://doi.org/10.1615/critrevbiomedeng.v32.i1.10

[12] E. Scalas, R. Gorenflo & F. Mainardi (2000). Fractional calculus and continuous-time finance. *Physica A: Statistical Mechanics and its Applications*, 284(1-4), 376–384. https://doi.org/10.1016/S0378-4371(00)00255-7

[13] R. P. Agarwal, A. M. A. El-Sayed & S. M. Salman (2013). Fractional-order Chua's system: discretization, bifurcation and chaos. *Advances in Difference Equations* , 2013, 320. https://doi.org/10.1186/1687-1847-2013-320

[14] Y. A. Rossikhin & M. V. Shitikova (1997). Application of fractional calculus to dynamic problems of linear and nonlinear hereditary mechanics of solids. *Applied Mechanics Reviews*, 50(1), 15–67. https://doi.org/10.1115/1.3101682

[15] U. Khan, R. Ellahi, R. Ullah, & et al. (2018). Correction to: extracting new solitary wave solutions of Benny-Luke equation and Phi-4 equation of fractional order by using (G'/G)-expansion method. *Optical and Quantum Electronics*, 50, 146. https://doi.org/10.1007/s11082-018-1421-4

[16] R. Ullah, R. Ellahi, S. M. Sait & S. T. Mohyud-Din (2020). On the fractional order model of HIV-1 infection of $CD4^+$ T-cells under the influence of antiviral drug treatment. *Journal of Taibah University for Science*, 14(1), 50–59. https://doi.org/10.1080/16583655.2019.1700676

[17] R. Ullah, R. Ellahi, S. T. Mohyud-Din & U. Khan (2018). Exact traveling wave solutions of fractional order Boussinesq-like equations by applying exp-function method. *Results in Physics*, 8, 114–120. https://doi.org/10.1016/j.rinp.2017.11.023

[18] A. Sohail, K. Maqbool & R. Ellahi (2018). Stability analysis for fractional-order partial differential equations by means of space spectral time Adams-Bashforth moulton method. *Numerical Methods for Partial Differential Equations*, 34(1), 19–29. https://doi.org/10.1002/num.22171

[19] J. P. C. Dos Santos, E. Monteiro & G. B. Vieira (2017). Global stability of fractional SIR epidemic model. In *Proceeding Series of the Brazilian Society of Computational and Applied Mathematics*, pp. 1–7. https://doi.org/10.5540/03.2017.005.01.0019

[20] H. A. A. El-Saka (2013). The fractional-order SIR and SIRS epidemic models with variable population size. *Mathematical Sciences Letters*, 2(3), 195–200. http://dx.doi.org/10.12785/msl/020308

[21] C. Vargas-De-León (2015). Volterra-type Lyapunov functions for fractional-order epidemic systems. *Communications in Nonlinear Science and Numerical Simulation*, 24(1-3), 75–85. https://doi.org/10.1016/j.cnsns.2014.12.013

[22] E. Ahmeda & A. S. Elgazzar (2007). On fractional order differential equations model for nonlocal epidemics. *Physica A: Statistical Mechanics and its Applications*, 379(2), 607–614. https://doi.org/10.1016/j.physa.2007.01.010

[23] D. Kiouach & Y. Sabbar (2021). Dynamic characterization of a stochastic SIR infectious disease model with dual perturbation. *International Journal of Biomathematics*, 14(4), 2150016. https://doi.org/10.1142/S1793524521500169

[24] E. Okyere, F. T. Oduro, S. K. Amponsah, I. K. Dontwi & N. K. Frempong (2016). Fractional order SIR model with constant population.*British Journal of Mathematics & Computer Science*, 14(2), 1–12. https://doi.org/10.9734/BJMCS/2016/23017

[25] M. F. Faraloya, S. Shafie, F. M. Siam, R. Mahmud & S. O. Ajadi (2021). Numerical simulation and optimization of radiotherapy cancer treatments using the Caputo fractional derivative. *Malaysian Journal of Mathematical Sciences* , 15(2), 161–187.

[26] Y. Guo (2017). The stability of the positive solution for a fractional SIR model.*International Journal of Biomathematics*, 10(1), 1750014. https://doi.org/10.1142/S1793524517500140

[27] P. A. Naik (2020). Global dynamics of a fractional order SIR epidemic model with memory. *International Journal of Biomathematics*, 13(8), 2050071. https://doi.org/10.1142/S1793524520500710

[28] M. Y. Li & J. S. Muldowney (1996). A geometric approach to global-stability problems. *SIAM Journal on Mathematical Analysis*, 27(4), 1070–1083. https://doi.org/10.1137/S0036141094266449

[29] X. Shi & Y. Cao (2020). Dynamics of a stochastic periodic SIRS model with time delay. *International Journal of Biomathematics*, 13(8), 2050072. https://doi.org/10.1142/S1793524520500722

[30] S. Zhao, Q. Lin, J. Ran, S. S. Musa, G. Yang, W. Wang & et al., (2020). Preliminary estimation of the basic reproduction number of novel coronavirus (2019-nCoV) in China, from 2019 to 2020: A data-driven analysis in the early phase of the outbreak. Int. J. Infect. Dis., 92, 214-P217.

[31] Zhao, S., Musa, S. S., Lin, Q., Ran, J., Yang, G., Wang, W.& et al. (2020). Estimating the unreported number of novel coronavirus (2019-nCoV) cases in China in the first half of January 2020: a data-driven modelling analysis of the early outbreak. *Journal of Clinical Medicine*, 9(2), 388.

[32] M. Dur-e-Ahmad & M. Imran (2020). Transmission dynamics model of coronavirus COVID-19 for the outbreak in most affected countries of the world. *International Journal of Interactive Multimedia and Artificial Intelligence*, 6, 7–10. http://dx.doi.org/10.9781/ijimai.2020.04.001

[33] K. Sarkar, S. Khajanchi & J. J. Nieto (2020). Modeling and forecasting the COVID-19 pandemic in India. *Chaos Solitons & Fractals*, 139, 110049. https://doi.org/10.1016/j.chaos.2020.110049

[34] S. Khajanchi, K. Sarkar, J. Mondal, S. N. Kottakkaran & S. F. Abdelwahab (2021). Mathematical modeling of the COVID-19 outbreak with intervention strategies. *Results in Physics*, 25, 104285. https://doi.org/10.1016/j.rinp.2021.104285

[35] S. Khajanchi & K. Sarkar (2020). Forecasting the daily and cumulative number of cases for the COVID-19 pandemic in India. *Chaos*, 30 (7), 071101. https://doi.org/10.1063/5.0016240

[36] P. Samui, J. Mondal, & S. Khajanchi (2020). A mathematical model for COVID-19 transmission dynamics with a case study of India. *Chaos Solitons & Fractals*, 140, 110173. https://doi.org/10.1016/j.chaos.2020.110173

[37] S. Khajanchi, K. Sarkar & Banerjee, S. (2022). Modeling the dynamics of COVID-19 pandemic with implementation of intervention strategies. *The European Physical Journal Plus*, 137, 129. https://doi.org/10.1140/epjp/s13360-022-02347-w

[38] Mondal J, S. Khajanchi (2022). Mathematical modeling and optimal intervention strategies of the COVID-19 outbreak. *Nonlinear Dynamics*, 109(1), 177–202. https://doi.org/10.1007/s11071-022-07235-7

[39] S. Khajanchi, B. Sovan & R. Tapan Kumar (2021). Mathematical analysis of the global dynamics of a HTLV-I infection model, considering the role of cytotoxic T-lymphocytes. *Mathematics and Computers in Simulation*, 180, 354–378. https://doi.org/10.1016/j.matcom.2020.09.009

[40] S. Khajanchi, S. Kankan, M. Jayanta, S. N. Kottakkaran & S. F. Abdelwahab (2021). Mathematical modeling of the COVID-19 pandemic with intervention strategies. *Results in Physics*, 25, 104285. https://doi.org/10.1016/j.rinp.2021.104285

[41] R. K. Rai, S. Khajanchi, P. K. Tiwari, E. Venturino & A. K. Misra (2022). Impact of social media advertisements on the transmission dynamics of COVID-19 pandemic in India. *Journal of Applied Mathematics and Computing*, 68, 19–44. https://doi.org/10.1007/s12190-021-01507-y

[42] B. Samia, S. Tareq, F. M. T. Delfim & Z. Anwar (2021). Control of COVID-19 dynamics through a fractional-order model.*Alexandria Engineering Journal*, 60(4), 3587–3592. https://doi.org/10.1016/j.aej.2021.02.022

[43] Y. G. Sanchez, Z. Sabir & J. L. G. Guirao (2020). Design of a nonlinear SITR fractal model based on the dynamics of a novel coronavirus (COVID-19). *Fractals*, 28(8), 2040026. https://doi.org/10.1142/S0218348X20400265

[44] A. R. Seadawy (2014). Stability analysis for Zakharov-Kuznetsov equation of weakly nonlinear ion-acoustic waves in a plasma. *Computers & Mathematics with Applications*, 67(1), 172–180. https://doi.org/10.1016/j.camwa.2013.11.001

[45] N. S. Ismail, N. M. Ariffin, R. Nazar & N. Bachok (2019). Stability analysis of stagnation-point flow and heat transfer over an exponentially shrinking sheet with heat generation. *Malaysian Journal of Mathematical Sciences*, 13(2), 107–122.

[46] N. A. Ahmad, N. Senu, Z. B. Ibrahim & M. Othman (2022). Stability analysis of diagonally implicit two derivative Runge-Kutta methods for solving delay differential equations. *Malaysian Journal of Mathematical Sciences*, 16(2), 215–235.

[47] A. R. Seadawy (2016). Stability analysis solutions for nonlinear three-dimensional modified Korteweg-de Vries-Zakharov-Kuznetsov equation in a magnetized electron-positron. *Plasma Physica A: Statistical Mechanics and its Applications*, 455, 44-51.

[48] A. A. Algaissi, N. K. Alharbi, M. Hassanain & A. M. Hashem (2020). Preparedness and response to COVID-19 in Saudi Arabia: Building on MERS experience. *Journal of Infection and Public Health*, 13(6), 834–838. https://doi.org/10.1016/j.jiph.2020.04.016

[49] H. Li, L. Zhang, C. Hu, Y. Jiang & Z. Teng (2016). Dynamical analysis of a fractional order predator-prey model incorporating a prey refuge. *Journal of Applied Mathematics and Computing*, 54, 435–449. https://doi.org/10.1007/s12190-016-1017-8

[50] A. Boukhouima, K. Hattaf & N. Yousfi (2017). Dynamics of a fractional order HIV infection model with specific functional response and cure rate. *Mathematical Modeling in Virology by Differential Equations*, 43, Article ID: 8372140, 8 pages. https://doi.org/10.1155/2017/8372140

[51] S. K. Choi, B. Kang & N. Koo (2014). Stability for Caputo fractional differential systems. *Abstract and Applied Analysis*, 2014, Article ID: 631419, 6 pages. https://doi.org/10.1155/2014/631419

[52] A. Hurwitz (1985). On the conditions under which an equation has only roots with negative real parts, *Mathematische Annelen*, 46, 273–284.

[53] J. P. LaSalle (1976). *The stability of dynamics systems*. SIAM, Philadelphia.

[54] P. Van den Driessche & J. Watmough (2002). Reproduction numbers and subthreshold endemic equilibria for compartmental models of disease transmission. *Mathematical Biosciences*, 180(1-2), 29–48. https://doi.org/10.1016/S0025-5564(02)00108-6

[55] J. Huo, H. Zhao & L. Zhu (2015). The effect of vaccines on backward bifurcation in a fractional order HIV model. *Nonlinear Analysis: Real World Applications*, 26, 289–305. https://doi.org/10.1016/j.nonrwa.2015.05.014